



**University of  
Zurich**<sup>UZH</sup>

**Zurich Open Repository and  
Archive**

University of Zurich  
University Library  
Strickhofstrasse 39  
CH-8057 Zurich  
[www.zora.uzh.ch](http://www.zora.uzh.ch)

---

Year: 2023

---

## **Constraining nonlinear time series modeling with the metabolic theory of ecology**

Munch, Stephan B ; Rogers, Tanya L ; Symons, Celia C ; Anderson, David ; Pennekamp, Frank

**Abstract:** Forecasting the response of ecological systems to environmental change is a critical challenge for sustainable management. The metabolic theory of ecology (MTE) posits scaling of biological rates with temperature, but it has had limited application to population dynamic forecasting. Here we use the temperature dependence of the MTE to constrain empirical dynamic modeling (EDM), an equation-free nonlinear machine learning approach for forecasting. By rescaling time with temperature and modeling dynamics on a “metabolic time step,” our method (MTE-EDM) improved forecast accuracy in 18 of 19 empirical ectotherm time series (by 19% on average), with the largest gains in more seasonal environments. MTE-EDM assumes that temperature affects only the rate, rather than the form, of population dynamics, and that interacting species have approximately similar temperature dependence. A review of laboratory studies suggests these assumptions are reasonable, at least approximately, though not for all ecological systems. Our approach highlights how to combine modern data-driven forecasting techniques with ecological theory and mechanistic understanding to predict the response of complex ecosystems to temperature variability and trends.

DOI: <https://doi.org/10.1073/pnas.2211758120>

Posted at the Zurich Open Repository and Archive, University of Zurich

ZORA URL: <https://doi.org/10.5167/uzh-252440>

Journal Article

Accepted Version

Originally published at:

Munch, Stephan B; Rogers, Tanya L; Symons, Celia C; Anderson, David; Pennekamp, Frank (2023). Constraining nonlinear time series modeling with the metabolic theory of ecology. *Proceedings of the National Academy of Sciences of the United States of America*, 120(12):e2211758120.

DOI: <https://doi.org/10.1073/pnas.2211758120>

1  
2  
3  
4  
5  
6  
7  
8  
9  
10  
11  
12  
13  
14  
15  
16  
17  
18  
19  
20  
21  
22  
23  
24  
25  
26  
27  
28  
29  
30

**Main Manuscript for**

**Constraining nonlinear time series modeling with the metabolic theory of ecology**

Stephan B. Munch<sup>1,2,\*</sup>, Tanya L. Rogers<sup>1</sup>, Celia C. Symons<sup>3</sup>, David Anderson<sup>4</sup>, Frank Pennekamp<sup>5,\*</sup>

<sup>1</sup> Southwest Fisheries Science Center, National Marine Fisheries Service, National Oceanic and Atmospheric Administration; Santa Cruz, CA 95060, USA

<sup>2</sup> Department of Applied Mathematics, University of California; Santa Cruz, Santa Cruz CA 95060, USA

<sup>3</sup> Department of Ecology and Evolutionary Biology, University of California; Irvine, Irvine CA 92697, USA

<sup>4</sup> Department of Zoology, University of British Columbia; Vancouver, BC V6T 1Z4, Canada

<sup>5</sup> Department of Evolutionary Biology and Environmental Studies, University of Zurich; Zurich 8057, Switzerland

\*Corresponding authors: Stephan B. Munch, Frank Pennekamp

**Email:** [smunch@ucsc.edu](mailto:smunch@ucsc.edu), [frank.pennekamp@ieu.uzh.ch](mailto:frank.pennekamp@ieu.uzh.ch)

**Author Contributions:** Conceptualization: SM; Methodology: SM, TR, DA; Investigation: SM, TR, CS, DA, FP; Visualization: TR, DA; Writing – original draft: SM, FP; Writing – review & editing: SM, TR, CS, DA, FP

**Competing Interest Statement:** Authors declare that they have no competing interests.

**Classification:** Biological Sciences/Ecology

**Keywords:** empirical dynamic modeling, population dynamics, thermal biology, physical–biological interactions

**This PDF file includes:**

- Main Text
- Figures 1 to 3
- Table 1

## 31 **Abstract**

32 Forecasting the response of ecological systems to environmental change is a critical challenge for  
33 sustainable management. The metabolic theory of ecology (MTE) posits scaling of biological rates with  
34 temperature, but it has had limited application to population dynamic forecasting. Here we use the  
35 temperature dependence of the MTE to constrain empirical dynamic modeling (EDM), an equation-free  
36 nonlinear machine learning approach for forecasting. By rescaling time with temperature and modeling  
37 dynamics on a 'metabolic timestep,' our method (MTE-EDM) improved forecast accuracy in 18 of 19  
38 empirical ectotherm time series (by 19% on average), with the largest gains in more seasonal  
39 environments. MTE-EDM assumes that temperature affects only the rate, rather than the form, of  
40 population dynamics, and that interacting species have approximately similar temperature dependence. A  
41 review of laboratory studies suggests these assumptions are reasonable, at least approximately, though  
42 not for all ecological systems. Our approach highlights how to combine modern data-driven forecasting  
43 techniques with ecological theory and mechanistic understanding to predict the response of complex  
44 ecosystems to temperature variability and trends.

## 45 **Significance Statement**

46 Forecasting how populations respond to climate change is an important challenge for natural resource  
47 managers. Forecasting approaches range from machine learning that is agnostic about underlying  
48 biological mechanisms to process-based models that incorporate mechanisms but are often complex and  
49 tailored toward specific species. Here we blend these approaches by constraining empirical dynamic  
50 modeling, a nonlinear machine learning approach, with the metabolic theory of ecology (MTE). Focusing  
51 on short-lived ectotherms with high-frequency sampling, the conditions in which our methodology is likely  
52 to be most effective, we obtained improved forecasts for most time series. This lends support to the MTE  
53 as a general predictive theory and provides a new tool with which to forecast abundances in  
54 environments with seasonal and/or inter-annual temperature change.

## 56 **Main Text**

### 58 **Introduction**

60 Forecasting the dynamics of ecosystems is a major challenge (1, 2), yet critical for the effective  
61 management of natural resources (3). More powerful methods, the increasing scale and resolution of  
62 ecological datasets, and advances in ecological theory can improve our ability to accurately forecast  
63 ecological systems, especially over the short term relevant for environmental decision-making (1).  
64 However, the complexity of natural ecosystems and the influence of numerous environmental drivers still  
65 pose a significant challenge to ecosystem forecasting, particularly in the face of ongoing environmental  
66 change (2).

67 Data-driven techniques such as machine learning have revolutionized forecasts of dynamical  
68 systems (4). However, a major drawback of these techniques is their limited ability to extrapolate to new  
69 conditions, as purely data-driven techniques perform poorly outside the historic envelope of variation (5).  
70 In contrast, mechanistic models can deal with changing conditions because they rely on mechanism,  
71 rather than past behavior, to extrapolate to previously unobserved conditions (6). Combining data-driven  
72 techniques with process-based models that obey mechanistic constraints could lead to better predictions  
73 of ecosystem dynamics. Blended models combine artificial intelligence and machine learning (e.g., deep  
74 neural networks) with process-based models to represent complex, integrated systems with many  
75 components and biophysical constraints (7). Thus, blended modeling approaches improve extrapolation  
76 by restricting data-driven predictions to those that follow physical laws (7). The potential for blending data-

77 driven and process-based forecasting has been recognized across various fields, including earth system  
78 science and medicine (8, 9), suggesting applications of this growing research area for ecology.

79 Empirical dynamic modeling (EDM) is a data-driven machine learning technique that has shown  
80 great promise in forecasting the dynamics of complex ecosystems (10, 11). The foundation of EDM is  
81 Takens' embedding theorem which states that lags of a single time series can reconstruct the dynamics  
82 of the complex, multidimensional system from which that series originated (12). Predictions are made by  
83 following nearby states (in delay coordinate space) forward in time, assuming that the past behavior of  
84 nearby states will reflect the future behavior of the system. EDM has been used successfully in many  
85 ecological applications where mechanistic models were lacking (11, 13, 14), and sometimes can even  
86 outperform forecasts made by fitting the 'correct' underlying mechanistic model (13). However, the fact  
87 that EDM does not require mechanism may also be a weakness – physical laws do not constrain its  
88 predictions, potentially resulting in implausible ecological states. Blending the EDM approach with first  
89 principles and biophysical constraints could improve forecasts.

90 For biological systems, temperature stands out as a major driver of processes such as enzymatic  
91 reactions, growth, reproduction, body size, and the pace of life, resulting in well-described patterns such  
92 as latitudinal and altitudinal diversity gradients (15, 16). Seasonal temperature fluctuations can be large,  
93 and due to climate change, global temperatures are expected to rise and show increased variability within  
94 and across regions over the coming century (17, 18). Shifting temperatures are already influencing the  
95 population dynamics of a wide range of taxa (19, 20), including pest species (21) and harmful algae (22);  
96 however, our ability to forecast the population-dynamic consequences of increasing temperatures across  
97 a wide range of organisms is still in its infancy.

98 The metabolic theory of ecology (MTE) is one of the few mechanistic ecological theories  
99 emerging from biophysical first principles (15). The MTE posits that biological rates, such as resting  
100 metabolic rate or growth rates, allometrically scale with body mass (with an exponent of  $3/4$ ) and for  
101 ectotherms, increase with temperature according to the Boltzmann factor (also known as the Arrhenius  
102 equation)  $e^{-E/kT}$  (where  $E$  is the activation energy and corresponds to a value of 0.65,  $k$  is Boltzmann's  
103 constant and  $T$  is temperature in Kelvin) (15). Endotherms, which can maintain a relatively constant body  
104 temperature, are not expected to show this same scaling of rates with environmental temperature. The  
105 effects of body size and temperature on individuals subsequently scale up to determine population-level  
106 properties (e.g., intrinsic rate of growth, carrying capacity, rate of extinction, or mortality) (15, 23, 24), and  
107 ecosystem properties like net ecosystem respiration (25). The MTE has outstandingly synthesized  
108 patterns across a wide range of scales from cell division to individual metabolism to macro-ecology (15,  
109 24, 26). However, most predictions of the MTE are for static, steady-state conditions.

110 The ability of the MTE to scale to higher-level processes suggests the theory could help forecast  
111 how temperature changes will affect population, community, and ecosystem dynamics. Indeed, models  
112 using the MTE have elucidated how population dynamic parameters scale with temperature (e.g., intrinsic  
113 rate of increase, carrying capacity, rate of extinction) (23, 24, 27, 28). The MTE has also successfully  
114 predicted within-host parasite dynamics across constant temperature environments (28). However, such  
115 detailed information on the temperature dependence of multiple vital rates is unavailable for most taxa,  
116 severely limiting our ability to forecast population dynamics under changing temperature conditions using  
117 mechanistic population models.

118 Here we blend EDM (a data-driven forecasting method) with the temperature dependence of the  
119 MTE to forecast population dynamics of a range of taxa under natural temperature fluctuations. Our  
120 predictive hybrid framework rescales time according to the MTE to achieve a constant 'metabolic'  
121 timestep: when temperatures are high, the metabolic timestep encompasses less calendar time; when  
122 temperatures are low, it encompasses more calendar time (**Fig. 1a,b**). Since empirically estimated  
123 activation energies deviate from the 'universal' average value of 0.65 (29), the activation energy used for  
124 this rescaling can either be specified or estimated from the data. In keeping with ecosystem applications  
125 of the MTE (e.g., 30, 31), we assume that the effect of temperature is *separable* (see Methods for a more

126 precise definition) from other influences on population dynamics. That is, temperature affects the overall  
127 rate of dynamics, not their form. Strictly speaking, this requires that all interacting species have similar  
128 thermal responses. Lack of separability could result from large variation in temperature dependence  
129 among interacting species and/or among different vital rates within a species. As an example, in a cyclic  
130 predator-prey system with separable temperature dependence, only the period of oscillations would  
131 change with temperature. As a counter-example, any system where a change in temperature causes a  
132 shift from oscillatory to equilibrium dynamics (e.g. 32) would lack separability. However, when thermal  
133 responses are similar across the observed range of temperatures, though not identical, we expect EDM  
134 with MTE temperature dependence to improve prediction relative to standard EDM, despite the lack of  
135 strict separability. If, in contrast, the separability assumption is strongly violated, the method will not work,  
136 which will be apparent in the lack of improvement. We examined the reasonableness of the separability  
137 assumption using existing laboratory data and tested the robustness of the method to variation in  
138 temperature dependence using simulations.

139 Using a collection of empirical field time series, we compared the EDM Simplex projection  
140 algorithm using a fixed calendar timestep (33) to Simplex projection using a metabolic timestep. For the  
141 metabolic timestep models, we used either the universal temperature dependence of 0.65 (the UTD  
142 model), temperature dependence estimated from the data (the MTE-EDM model), or for 3 species for  
143 which we could obtain data, temperature dependence based on empirical thermal performance curves  
144 (the TPC model). For comparison, we also fit a calendar timestep model with temperature as a covariate,  
145 which is a common alternative approach for incorporating temperature into EDM (34, 35).

## 146 147 **Results**

148  
149 We first tested whether the temperature separability assumption is reasonable using data from  
150 published laboratory experiments measuring population dynamics across a gradient of constant  
151 temperatures. The pace of population dynamics, measured by log cycle period, displayed temperature  
152 scaling consistent with the MTE in three species (**Fig. 1c, S1, Table S1**). The scaling exponent for the  
153 rotifer *Brachionus calyciflorus* was 0.57 (95% CI: 0.22-0.93,  $R^2=0.83$ ) (36), and exponents for the  
154 predator-prey pair *Didinium nasutum* and *Paramecium caudatum* were 0.68 (95% CI: 0.39-0.97,  $R^2=0.95$ )  
155 and 0.67 (95% CI: 0.37-0.97,  $R^2=0.91$ ), respectively (37). However, we did not find the expected scaling  
156 relationship in two additional studies: a *Tetrahymena pyriformis*-*Pseudomonas fluorescens* predator-prey  
157 system (38) and the moth *Plodia interpunctella* (39). In the latter studies, temperature likely drove those  
158 systems across bifurcations that qualitatively changed their dynamics instead of only influencing the rate  
159 of change. Thus, while it is clear that not all systems meet the assumptions of MTE-EDM, for systems that  
160 do, we would expect the method to produce forecasting improvements in environments with temperature  
161 variation.

162 As a proof of concept, we simulated a chaotic three species food chain (40) under two  
163 temperature change scenarios: a linear temperature increase (**Fig. S2a**), and a more realistic scenario  
164 with seasonal temperature variation (26°C), a long-term trend (~1.5°C over 10 years), and stochasticity  
165 (**Fig. 2a**). In both scenarios, Simplex that does not account for temperature change results in poor  
166 predictive performance ( $R^2 < 0.2$ ), even as the embedding dimension (number of lags used) was  
167 increased (**Fig. 2b, S1b**). MTE-EDM greatly improved performance over Simplex ( $R^2 > 0.8$ , **Fig. 2b, S2b**)  
168 and use of the dynamic timestep improved the resolution of the reconstructed underlying attractor, which  
169 was otherwise distorted by temperature-dependent dynamics (**Fig. 2c,d, S1c,d**). These simulations also  
170 demonstrate the effectiveness of MTE-EDM when temperature is nonstationary and shows directional  
171 trends.

172 To explore sensitivity of MTE-EDM to variation in species-specific responses to temperature, we  
173 ran additional multi-species simulations with variable numbers of interacting ecto- and endotherms, for  
174 which the ectotherms had variable activation energies (**Fig. S3, S4**). Although MTE-EDM is applied to

175 data from a single species, the estimated activation energy integrates the temperature dependence of all  
176 closely interacting species, and variation in temperature dependence among species makes the  
177 population dynamics non-separable from temperature. Results show that in ectotherm-dominated  
178 systems, MTE-EDM is robust to variation in activation energy, recovering the correct mean activation  
179 energy in the presence of considerable variation among species. MTE-EDM frequently outperformed  
180 Simplex, particularly as the mean activation energy increased and variability in the activation energy  
181 among species decreased. The exception, not surprisingly, was when most community members were  
182 endotherms, in which case the mean activation energy estimate was biased low, and performance did not  
183 improve notably over Simplex. Thus, the method is robust to modest violations of the assumption of strict  
184 separability.

185 We next evaluated whether MTE-EDM improves prediction in field populations exposed to natural  
186 temperature fluctuations. We assembled a database of 22 time series from 8 locations (5 aquatic, 3  
187 terrestrial) spanning a range of taxa (e.g. phytoplankton, crustaceans, moths, rodents; **Table 1, S2**).  
188 Sampling intervals ranged from half-weekly to monthly, and mean temperatures ranged from 9.8 to  
189 26.7°C. Absolute forecasting skill for both Simplex and MTE-EDM was high across time series, with  $R^2$   
190 values ranging from 0.22 to 0.85 (mean: 0.60) for Simplex and 0.39 to 0.88 (mean: 0.67) for MTE-EDM  
191 (**Table 1**). For 18 of 19 ectotherm time series, MTE-EDM outperformed Simplex, increasing forecast skill  
192 of these 18 series by 20% on average (19% across all series, **Fig. 3a**). Likelihood ratio tests indicated  
193 that this improvement was statistically significant in 17 of 19 cases. In terms of  $R^2$  values, MTE-EDM  
194 outperformed UTD in all cases, and UTD outperformed Simplex in only 8 of 19 cases. Using temperature  
195 as a covariate outperformed Simplex in 14 cases, but outperformed MTE-EDM in only 3 cases. Estimated  
196 activation energies from MTE-EDM were within the range of values estimated in other studies (29) and  
197 did not approach the parameter bounds (**Fig. 3c, S5**). As expected, MTE-EDM resulted in little forecast  
198 improvements for 3 endotherm time series (0.8% on average, **Fig. 3a**). The estimated activation energies  
199 for the endotherm series were close to 0, and the use of UTD decreased performance.

200 Seasonality was the dominant source of temperature variability in our field time series (trend: 0 -  
201 2.8°C year<sup>-1</sup> [median 0.04]; seasonal range: 1.4 - 24°C [median 19]), as is typical of temperatures  
202 throughout most of the world (41). Among ectotherms, the degree of improvement when using MTE-EDM  
203 was strongly related to the seasonality of the environment, with larger improvement in forecast skill in  
204 more variable environments (**Fig. 3b**). This is a sensible result: If there is little variation in temperature,  
205 there will also be little variation in the length of the metabolic timestep, and thus the MTE-EDM model will  
206 be similar to Simplex.

207 Despite the MTE's success in explaining large-scale biological patterns in relation to  
208 environmental temperature, physiologists have pointed out that the MTE's monotonic increase of vital  
209 rates with temperature is unrealistic (29). Thermal performance curves (TPCs) are usually domed: vital  
210 rates increase with temperature up to an optimum temperature and then decrease rapidly beyond the  
211 optimum (42). Organisms are typically exposed to a range of temperatures, including sub-optimal  
212 temperatures, especially in seasonal environments (43). Our modeling framework can readily use a TPC  
213 instead of MTE temperature scaling to determine the length of the metabolic timestep, which we expect to  
214 produce better results when the organism often experiences temperatures on the descending limb of the  
215 TPC. We obtained TPCs for the three species in our time series database for which curves were available  
216 and tested whether TPC-based models could improve forecasts. We found that forecasting skill was  
217 worse than MTE-EDM in all cases and worse than Simplex in 2 cases (**Fig. 3a**).

## 218 219 **Discussion**

220  
221 Previous work on EDM has shown that unequally spaced lags can be optimal for modeling  
222 systems with multiple timescales (44) and that in 'driven' systems, delays of the driver (in this case  
223 temperature) included as additional predictors (covariates) can improve the forecast performance (45).

224 However, Takens' theorem (12) shows that adding lags of temperature to an EDM model also adds  
225 information from other variables that interact with temperature, making a mechanistic interpretation  
226 difficult. For instance, (35) found that the temperature dependence at lag 1 was unimodal or increasing  
227 (as expected for thermal performance) but was bowl-shaped or decreasing at lag 2, possibly representing  
228 an indirect effect through predation or competition. Here we show that constraining EDM to obey a known  
229 mechanism outperforms the covariate approach in the majority of cases. Additionally, using a metabolic  
230 time step adds only one degree of freedom to the model, and permits model comparison to Simplex with  
231 a simple likelihood ratio. In contrast, the change in degrees of freedom that results from adding  
232 temperature as an additional coordinate in the nonparametric Simplex model is difficult to determine *a*  
233 *priori*, rendering a likelihood ratio test inappropriate for comparing this model. Our study is the first  
234 demonstration that separable, nonautonomous dynamics can be embedded through a simple time scale  
235 change.

236 Not all biological rates or organisms have the same temperature dependence (29, 46, 47), and  
237 allowing for variable activation energies improved performance over the 'universal' value of 0.65.  
238 Surprisingly, MTE-EDM's temperature scaling performed better than scaling using empirical TPCs,  
239 despite the known unimodal shape of thermal performance (48). This could be because most  
240 temperatures experienced by the focal species were below the TPC optimum. Additionally, different  
241 biological processes have different TPCs (29), and the particular one measured may or may not reflect  
242 the temperature dependency of the population dynamics, which integrates across many biological  
243 processes and interacting species (49). However, since only 3 species had TPCs, more applications are  
244 needed before we can draw any general conclusions about the performance of this method relative to  
245 MTE-EDM.

246 Of course, temperature is not the only factor affecting biological rates or population dynamics,  
247 which may explain why MTE-EDM did not always greatly improve forecast skill, even with ample  
248 temperature variation. Understanding whether there are general rules for how temperature scaling shifts  
249 when resources are limiting is an active area of research, and testing whether the patterns described in  
250 the literature can be used as constraints to improve forecasts would be a useful direction for future  
251 forecasting research. For example, ecological stoichiometry posits that phosphorus content directly  
252 influences the growth rates of aquatic organisms (50). Ongoing efforts to expand the metabolic theory to  
253 include important constraints such as stoichiometry (e.g., 50, 51) could mean that additional adjustments  
254 to the metabolic time step may be possible (e.g. based on phosphorus availability (52)). However, not all  
255 environmental factors influence biological rates in a known or universal way that is separable from other  
256 population dynamics, as assumed in MTE-EDM, so there is not necessarily a straightforward way to  
257 integrate them into the metabolic time step. In these cases, environmental variables could be covariates  
258 rather than constraints or indirectly captured by the time lags. Coupling EDMs with physical models is  
259 another approach to incorporating mechanism that has been recently explored. For instance, EDM has  
260 recently been used in a hybrid modeling approach where data-driven predictions of the biogeochemical  
261 components of Lake Geneva were combined with a model of lake physics to predict future lake health  
262 (53). This yielded better forecast performance for dissolved oxygen concentration than the physical  
263 model. Blending data-driven methods with theory therefore provides new avenues to both improve  
264 forecasts and increase our understanding of relevant mechanisms.

265 When using MTE-EDM, practitioners must consider the timescale of the system they are  
266 modeling and the resolution of the population and temperature data available. First, MTE-EDM needs  
267 samples taken frequently enough to be able to construct uniform metabolic time steps. Sampling intervals  
268 that are too coarse limit our ability to do so. Second, MTE-EDM requires sufficient temperature variation  
269 on timescales relevant to the focal organism. For example, in all of our field time series, the focal  
270 organisms all had relatively short generation times, often less than the annual temperature cycle,  
271 resulting in temperature variation across generations. In contrast, population dynamics of species with  
272 generation times  $\gg 1$  year should be relatively insensitive to seasonal fluctuations in temperature

273 because from one generation to the next, the mean temperature will be more or less the same. Long-lived  
274 species may be sensitive to interannual variation in temperature (including climate change), but since this  
275 variation is typically much less than seasonal temperature variation (e.g.  $\sim 2^{\circ}\text{C}$  over the past hundred  
276 years versus  $20^{\circ}\text{C}$  within a year), it may only be apparent over very long timescales. Hence, the  
277 effectiveness of MTE-EDM will depend on the generation time of the organism, the observed temperature  
278 range, and the availability of data. At present, we expect MTE-EDM to be most effective for ectotherms  
279 with short generation times ( $\sim 1$  year or less) and high frequency sampling (at least monthly). That said,  
280 we note that the change of variables used here is generic - any driver with approximately separable  
281 effects on dynamics could be built into EDM in this way.

282 Although MTE-EDM improved forecasts in the series we analyzed and our simulations indicated  
283 that MTE-EDM is robust to modest variation in activation energy among interacting ectotherms, it is worth  
284 noting conditions under which MTE-EDM will not improve forecasts. MTE-EDM will not improve forecasts  
285 when there is little variation in temperature, or when most interacting species are insensitive to  
286 temperature (e.g. endotherms). Less obviously, MTE-EDM is not expected to work when the separability  
287 assumption is strongly violated (e.g. where vital rates within and across species have sufficiently different  
288 effects over the observed range of temperatures). In particular, it will not improve forecasts when the lack  
289 of separability results in temperature driven shifts in structural stability, as occurs in some models (30,  
290 51), experimental systems (36), and field systems (e.g. tea tortrix moth (52)). The prevalence of such  
291 temperature-driven bifurcations in natural systems under current climate conditions is an open question.  
292 On the other hand, in cases where the temperature does vary, a failure of MTE-EDM to improve  
293 performance over Simplex suggests that either the system is temperature-independent (activation energy  
294 near 0) or that nonseparability is present. So, although we do not expect the MTE-EDM approach to be  
295 useful in all systems, its failure suggests alternative hypotheses that are worth exploring.

296 Although we did not see this in our data and have insufficient sample size to draw any general  
297 conclusions, we suspect MTE-EDM might work better on aggregated time series, since species-specific  
298 temperature dependencies may average out. Aggregation has also been shown to lead to higher forecast  
299 accuracy with EDM (54).

300 EDM – and other data-driven approaches – are powerful tools for making predictions and gaining  
301 insights into complex systems. Their power comes from their generality – we don't need to know how a  
302 system works for them to be useful. However, one of the strengths of mechanistic model building is that  
303 known mechanisms and auxiliary data (not time series) are readily incorporated. Several previous studies  
304 have noted the importance of bringing together empirical and mechanistic approaches (8, 55–57). Our  
305 approach is a novel addition to this growing toolbox. For systems that meet the assumptions of the  
306 method, it offers a new way to account for temperature variability and nonstationarity both now and in a  
307 future increasingly influenced by climate change.

308



309 **Materials and Methods**

310

311 ***Time delay embedding***

312

313 Time delay embedding refers to the reconstruction of system dynamics using time lags of one or  
314 more variables from that system. For a generic, autonomous dynamical system of dimension  $S$ ,

315 
$$dx_i/dt = f_i(x_1, \dots, x_S) \quad [1]$$

316 that converges to an attractor with dimension  $d < S$ , Takens proved that the lag vectors  $X_i(t) =$

317  $\{x_i(t), x_i(t + \tau), \dots, x_i(t + E\tau)\}$  are sufficient to embed the attractor, where  $\tau$  is a time delay and  $E + 1$  is

318 the embedding dimension (12). For the remainder, we do this for each time series independently and

319 drop the subscript  $i$  to simplify the notation. The practical upshot of Takens' theorem is that we can model

320 the next state,  $x(t)$ , as

321 
$$x(t) = F(x(t - \tau), \dots, x(t - E\tau)) \quad [2],$$

322 where one of several function approximation schemes can be used to estimate the delay embedding  
323 map,  $F$ , from time series data. The simplest such scheme is the nearest neighbor approach, referred to

324 in ecology as the Simplex projection algorithm (33, 58). To make a prediction for  $x(t)$ , Simplex uses the

325 averages of the  $E + 1$  nearest neighbors of  $\{x(t - \tau), \dots, x(t - E\tau)\}$ . Although there have been many

326 elaborations on this approach, Simplex makes the fewest assumptions and has the fewest tunable

327 parameters. As such, it is a natural benchmark for generalization.

328

329 ***Rescaling time with temperature (metabolic embedding)***

330

331 The MTE posits that the effect of temperature ( $T$ ) on metabolism structures fecundity and

332 mortality rates, and hence species interactions. Within ectotherms, the activation energy is highly

333 conserved. Under these assumptions, the population dynamics of the  $i$ th species are given approximately

334 by

335 
$$dx_i/dt = f_i(x_1, \dots, x_S, T) \approx f_i(x_1, \dots, x_S)h(T) \quad [3]$$

336 where  $h(T)$  is the average temperature dependence and  $f_i$  describes the effects of all other state

337 variables. This approximation assumes the population and temperature dynamics are separable, such

338 that temperature primarily affects the overall rate of change, and that all species approximately adhere to

339 the same universal temperature dependence. This is clearly not exactly true for most real systems and we

340 evaluate the consequence of deviations using simulations.

341 System [3] falls under the skew-product embedding theorems of Stark (45), which would expand

342 the delay coordinate space to include lags of temperature in a nonparametric way. This is the justification

343 for using temperature as an additional coordinate (covariate) in the Simplex model. However, including

344 temperature in this way does not explicitly take advantage of the known functional dependence on

345 temperature, i.e.  $h(T) = e^{-E_0/kT}$  where  $k = 8.617 \times 10^{-5} eV/K$  is Boltzmann's constant,  $T$  is temperature

346 in degrees Kelvin, and  $E_0$  is the activation energy.

347 Here, we make use of both the separability implied by equation [3] and the fact that  $h(T)$  is

348 known, to introduce a metabolic time,  $\mu$ , which renders the dynamics autonomous. Specifically, if  $d\mu/dt =$

349  $h(T)$ , then  $dx_i/d\mu = f_i(x_1, \dots, x_S)$ , eliminating the need for skew-product embedding. Integrating over a

350 fixed  $\mu$ -step, we obtain a discrete  $\mu$  model

351 
$$x_{i,n} = F_i(x_{i,n-1}, \dots, x_{S,n-1})$$

352 where  $x_{i,n} = x_i(t_n)$  and the times  $t_n$  are defined implicitly by  $\int_0^{t_n} h(T) = n\mu$ . From here, Takens theorem

353 allows us to re-cast the dynamics as

354 
$$x_n = \tilde{F}(x_{n-1}, x_{n-2}, \dots, x_{n-E})$$

355 where we have again dropped the subscript  $i$  to simplify the notation though we remind the reader that

356 the inputs to  $\tilde{F}$  are lags of a single state variable.

357 If data were available in continuous time, we would construct delay vectors for each  $x(t_n)$  such  
 358 that  $\int_{t_{n-j}}^{t_n} h(T)dt = j\mu$  exactly. In practice, however, data are available on a discrete time step so some  
 359 approximation is necessary. For simplicity, we find the sampling times  $t_{n-j}$  such that  $\sum_{t_{n-j}}^{t_n} h(T_i)\Delta t$  is as  
 360 close to  $j\mu$  as possible. Given the collection of metabolic delay vectors, we use the same nearest-  
 361 neighbor averaging to approximate  $\tilde{F}$  that we used for the Simplex algorithm.

362 Although  $E_0=0.65$  has been referred to as ‘universal temperature dependence’ (UTD) (15),  
 363 subsequent meta-analyses (29) found substantial variability in  $E_0$  across species and traits. For MTE-  
 364 EDM, we, therefore, estimate  $E_0$  by computing the log likelihood on a grid of 50 values of  $E_0$  from 0 to 2  
 365 and a maximum embedding dimension of 15. In keeping with other EDM studies that minimize squared  
 366 prediction errors, a Gaussian likelihood was used. Note that UTD ( $E_0= 0.65$ ) and Simplex ( $E_0= 0$ ) are  
 367 special cases of MTE-EDM, so that twice the log likelihood ratio is expected to follow a chi-square  
 368 distribution with one degree of freedom. It is less clear how the degrees of freedom change when using  
 369 temperature as an additional coordinate, so significance levels for the likelihood ratio test are approximate  
 370 in this case. Although MTE-EDM is applied to data for a single species, it is important to recognize that  
 371 the estimated  $E_0$  represents an average for the species with which it closely interacts, rather than a  
 372 species-specific metabolic rate.

### 373 **Simulated data**

374 As a proof of concept, we simulated a chaotic three species food chain (40) in which the vital  
 375 rates depend on temperature as in equation [3]. Specifically, we used

$$\begin{aligned}
 376 \quad \frac{dx}{dt} &= h(T)[x(1-x) - axy/(1+bx)] \\
 377 \quad \frac{dy}{dt} &= h(T)[axy/(1+bx) - cyz/(1+dy) - my] \\
 378 \quad \frac{dz}{dt} &= h(T)[cyz/(1+dy) - \mu z]
 \end{aligned}$$

382 where  $a = 5.0, b = 3.0, c = 0.1, d = 2.0, m = 0.4, \mu = 0.01$  and the initial conditions were  $x(0) = 0.8, y(0) =$   
 383  $0.1, z(0) = 9.0$ . The system was integrated using a 4th order Runge-Kutta scheme on a weekly time step  
 384 for 500 weeks. To provide interesting test cases, we simulated a temperature trend,  $T(t) = 0.052t - 8$ ,  
 385 and a more realistic scenario with seasonal temperature variation, a long-term trend, and stochasticity,  
 386  $T(t) = 5 + 13 \sin(2\pi t/55) + 0.003t + 2.6\epsilon(t)$  where  $\epsilon(t) \sim N(0,1)$  is white noise. The linear increase of  
 387  $0.003^\circ\text{C week}^{-1}$  results in a net increase of  $1.5^\circ\text{C}$  over the  $\sim 10$  year simulation.

388 To understand the effect of variable activation energies within a community, we also simulated 10  
 389 years of weekly data using the food chain model described above, but with  $h(T)$  allowed to vary among  
 390 species- violating the assumption of strict system-level separability. We considered four scenarios: 1) two  
 391 ectotherms, 2) three ectotherms, 3) two ectotherms and one endotherm, and 4) one ectotherm and two  
 392 endotherms. For each ectotherm we generated random activation energies drawn from a Gaussian  
 393 distribution with different means (0.20, 0.32, 0.65, 1.20) representing most of the typically observed range  
 394 crossed with three levels of variability (SD: 0, 0.1, 0.2). Note that the interval 0.2 to 1.2 was originally  
 395 proposed for variation in activation energy (26) and provided good bounds for within-species variation in  
 396 lifespan (59), while 0.32 and 0.65 are typical values for photosynthesis and ectotherm metabolism,  
 397 respectively.

398 For each of the 4 scenarios, 4 mean activation energies, and 3 SDs, we ran 50 replicates from  
 399 random initial conditions for a total of 2400 simulated data sets. For each data set, we used the MTE-  
 400

401 EDM approach to estimate the activation energy and used likelihood ratio tests to assess the probability  
402 that MTE-EDM would be significantly better than Simplex.

403

#### 404 ***Analysis of empirical data***

405

##### 406 *Cycle period in lab experiments*

407 To examine the impact of temperature on population cycle period, we searched the literature for  
408 laboratory experiments reporting population dynamics at different constant temperatures. This search  
409 yielded four studies: a rotifer (*Brachionus calyciflorus*) population (36), a ciliate (*Didinium-Paramecium*)  
410 predator-prey system (37), a moth (*Plodia interpunctella*) (39), and a ciliate-bacteria (*Tetrahymena*  
411 *pyriformis-Pseudomonas fluorescens*) predator-prey system (38). Raw data were obtained from  
412 supplementary materials or, if necessary, directly from figures using WebPlotDigitizer (60).

413 We used spectral analysis to assess the periodicity for each abundance time series. To compute  
414 the power spectrum, we used penalized (ridge) regression onto sine and cosine basis functions with  
415 frequencies  $2\pi s/N$ , where  $s = 2, 3, \dots, N/2$  and  $N$  is the time series length (thus, the longest period  
416 considered was  $0.5N$ , and the shortest was 2 timesteps). Time series were rescaled to mean 0 and unit  
417 variance prior to analysis, and the penalty was set to 0.01. Power at each frequency was calculated from  
418 the sine and cosine coefficients. The frequency (cycle period) with the highest power was then selected.  
419 For (38), we performed analyses on the average abundance at each time point and excluded replicate A  
420 for *Tetrahymena pyriformis* because the density was 0 throughout the time series. For (37), visual  
421 inspection of the time series showed that *Didinium* and *Paramecium* each went through one cycle before  
422 going extinct. Thus, we computed cycle period as the length of time to extinction. The *Didinium* population  
423 at 17°C did not finish its cycle (i.e., it did not go extinct) during the experiment, so was excluded.

424 We performed ordinary least squares regression to assess the relationship between natural log-  
425 transformed cycle period and inverse absolute temperature, i.e.,  $1/kT$ , where  $k$  is Boltzmann's constant.  
426 The slope of this relationship corresponds to the activation energy.

427

##### 428 *Natural population dynamics*

429 To evaluate the MTE temperature effect on natural populations, we assembled a database of  
430 time series from 22 short-lived species from terrestrial and aquatic environments (**Table 1, Table S2**). We  
431 chose to focus on species with sub-annual sampling intervals and short generation times in order to  
432 encompass seasonal variation in temperature and ensure sufficient data to reconstruct dynamics. Most  
433 time series were species-level, although 4 time series represented species aggregates (e.g.,  
434 phytoplankton). Sampling intervals ranged from 3 days to 1 month, and sampling time ranged from 2 to  
435 40 years. Temperature data were either recorded during sample collection or obtained from nearby  
436 sources (**Table S2**). If a database contained multiple species, for our proof-of-concept purposes, we  
437 analyzed the 5-6 most abundant species with the longest continuous records. We also excluded series if  
438 the Simplex algorithm had prediction  $R^2$  less than 0.2.

439 Each abundance time series was square-root transformed and standardized to zero mean and  
440 unit standard deviation prior to analysis. Since the sampling interval was somewhat variable for many of  
441 the time series, series were interpolated to the shortest constant interval (3-day, weekly, bi-weekly, or  
442 monthly) that was most consistent with the original sampling scheme using a Gaussian process  
443 regression with a cyclic prior mean with Fourier modes at  $2^s$  years where  $s = -2, -1, 0, 1, 2, 3$ .  
444 Temperature data were interpolated similarly, but were not square-root transformed.

445 For each time series, we fit 2 calendar timestep models (standard Simplex, temperature as a  
446 covariate), and 2 metabolic timestep models (UTD, MTE-EDM). For the calendar timestep models, we  
447 selected the pair of embedding dimension and time delay,  $\tau$ , that maximized forecast accuracy: We  
448 evaluated embedding dimensions ranging from 1 to 5, and time delays ranging from 1 to 12 steps, where  
449 the step size was set by the original sampling scheme. For the metabolic timestep models, we selected

450 the embedding dimension that maximized forecast accuracy, fixing the metabolic delay,  $\mu$ , to the average  
451 metabolism over the same time step. That is, if the time series was sampled weekly, for a total of  $N$   
452 weeks, we set  $\mu = \frac{1}{N} \sum_i e^{-0.65/kT_i}$ . Forecast accuracy was measured using leave-one-out prediction  $R^2$ ,  
453 excluding the time point before and after, which was also used as our measure of forecast performance.  
454 While alternative cross-validation schemes or performance measures may give different results in terms  
455 of absolute forecast skill, the relative performance of the different models should be the same.

456 To evaluate the effect of thermal performance curve (TPC) shape on metabolic embedding, we  
457 obtained empirical TPCs for two copepod species (*Acartia tonsa*, *Acartia hudsonica*) and the tea tortrix  
458 moth (*Adoxophyes honmai*). TPCs for the copepods were obtained by fitting a Sharpe-Schoolfield model  
459 (61) to egg production data for each copepod species (62). For *Adoxophyes honmai*, we fit the same  
460 model to laboratory data for lifetime production of hatching eggs, calculated from data for age-specific  
461 survival, fecundity, and egg hatchability (63). TPCs were unavailable for the other species for which we  
462 had time series.

463

## 464 **Acknowledgments**

465

466 The University of Zurich Research Priority Program on Global Change and Biodiversity supported this  
467 research. We thank the two anonymous reviewers for their constructive comments and suggestions,  
468 which have considerably improved the methodology and manuscript.

469

## 470 **Funding**

471

472 FP was supported by the Swiss National Science Foundation (grant 310030\_197811). CCS was  
473 supported by a Hellman Fellowship Award at the University of California, Irvine.

474

## 475 **Data and Code Availability**

476

477 The laboratory time series, interpolated field time series, and all code required to reproduce the analyses  
478 are available at [https://github.com/tanyalrogers/MTE\\_EDM](https://github.com/tanyalrogers/MTE_EDM). Field data sources are listed in **Table S2**. The  
479 datasets used for Lake Geneva are © OLA-IS, AnaEE-France, INRAE of Thonon-les-Bains, CIPEL,  
480 citation in Table S2.

## 481 **References**

- 482 1. M. C. Dietze, *et al.*, Iterative near-term ecological forecasting: Needs, opportunities, and  
483 challenges. *Proc. Natl. Acad. Sci.* **115**, 1424–1432 (2018).
- 484 2. J. S. Clark, *et al.*, Ecological Forecasts: An Emerging Imperative. *Science* **293**, 657–660  
485 (2001).
- 486 3. D. E. Schindler, R. Hilborn, Prediction, precaution, and policy under global change.  
487 *Science* **347**, 953–954 (2015).
- 488 4. S. L. Brunton, J. L. Proctor, J. N. Kutz, Discovering governing equations from data by  
489 sparse identification of nonlinear dynamical systems. *Proc. Natl. Acad. Sci.* **113**, 3932–  
490 3937 (2016).
- 491 5. J. Elith, J. R. Leathwick, Species Distribution Models: Ecological Explanation and  
492 Prediction Across Space and Time. *Annu. Rev. Ecol. Evol. Syst.* **40**, 677–697 (2009).

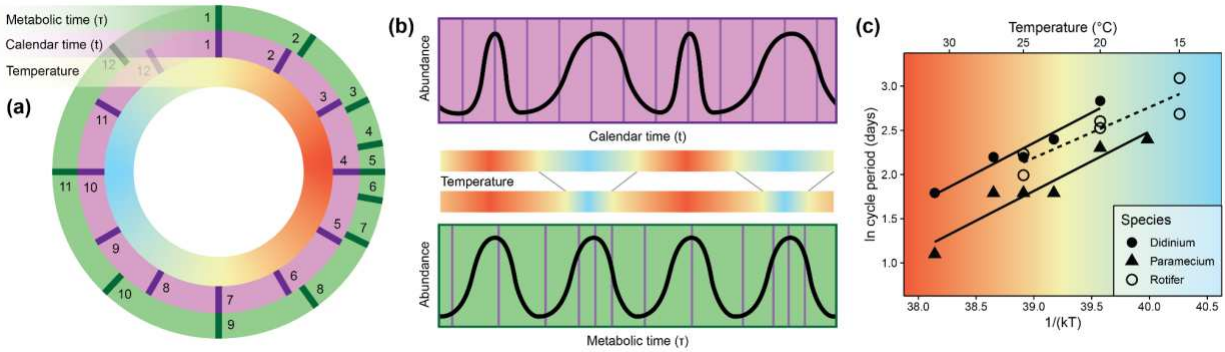
- 493 6. O. L. Petchey, *et al.*, The ecological forecast horizon, and examples of its uses and  
494 determinants. *Ecol. Lett.* **18**, 597–611 (2015).
- 495 7. L. Parrott, Hybrid modelling of complex ecological systems for decision support: Recent  
496 successes and future perspectives. *Ecol. Inform.* **6**, 44–49 (2011).
- 497 8. M. Reichstein, *et al.*, Deep learning and process understanding for data-driven Earth  
498 system science. *Nature* **566**, 195–204 (2019).
- 499 9. M. Alber, *et al.*, Integrating machine learning and multiscale modeling—perspectives,  
500 challenges, and opportunities in the biological, biomedical, and behavioral sciences. *Npj*  
501 *Digit. Med.* **2**, 1–11 (2019).
- 502 10. H. Ye, G. Sugihara, Information leverage in interconnected ecosystems: Overcoming the  
503 curse of dimensionality. *Science* **353**, 922–925 (2016).
- 504 11. H. Ye, *et al.*, Equation-free mechanistic ecosystem forecasting using empirical dynamic  
505 modeling. *Proc. Natl. Acad. Sci.* **112**, E1569–E1576 (2015).
- 506 12. F. Takens, “Detecting strange attractors in turbulence” in *Dynamical Systems and*  
507 *Turbulence, Warwick 1980*, Lecture Notes in Mathematics., D. Rand, L.-S. Young, Eds.  
508 (Springer, Berlin, Heidelberg, 1981), pp. 366–381.
- 509 13. C. T. Perretti, S. B. Munch, G. Sugihara, Model-free forecasting outperforms the correct  
510 mechanistic model for simulated and experimental data. *Proc. Natl. Acad. Sci.* **110**, 5253–  
511 5257 (2013).
- 512 14. C. Karakoç, A. T. Clark, A. Chatzinotas, Diversity and coexistence are influenced by time-  
513 dependent species interactions in a predator–prey system. *Ecol. Lett.* **23**, 983–993 (2020).
- 514 15. J. H. Brown, J. F. Gillooly, A. P. Allen, V. M. Savage, G. B. West, Toward a metabolic  
515 theory of ecology. *Ecology* **85**, 1771–1789 (2004).
- 516 16. B. A. Hawkins, *et al.*, A Global Evaluation of Metabolic Theory as an Explanation for  
517 Terrestrial Species Richness Gradients. *Ecology* **88**, 1877–1888 (2007).
- 518 17. M. Collins, *et al.*, Long-term Climate Change: Projections, Commitments and Irreversibility.  
519 *Clim. Change 2013 - Phys. Sci. Basis Contrib. Work. Group Fifth Assess. Rep. Intergov.*  
520 *Panel Clim. Change*, 1029–1136 (2013).
- 521 18. G. A. Meehl, C. Tebaldi, More Intense, More Frequent, and Longer Lasting Heat Waves in  
522 the 21st Century. *Science* **305**, 994–997 (2004).
- 523 19. A. J. Davis, L. S. Jenkinson, J. H. Lawton, B. Shorrocks, S. Wood, Making mistakes when  
524 predicting shifts in species range in response to global warming. *Nature* **391**, 783–786  
525 (1998).
- 526 20. E. Post, M. C. Forchhammer, Synchronization of animal population dynamics by large-  
527 scale climate. *Nature* **420**, 168–171 (2002).

- 528 21. K. J. Haynes, A. J. Allstadt, D. Klimetzek, Forest defoliator outbreaks under climate  
529 change: effects on the frequency and severity of outbreaks of five pine insect pests. *Glob.*  
530 *Change Biol.* **20**, 2004–2018 (2014).
- 531 22. M. L. Wells, *et al.*, Harmful algal blooms and climate change: Learning from the past and  
532 present to forecast the future. *Harmful Algae* **49**, 68–93 (2015).
- 533 23. V. M. Savage, J. F. Gillooly, J. H. Brown, G. B. West, E. L. Charnov, Effects of body size  
534 and temperature on population growth. *Am. Nat.* **163**, 429–441 (2004).
- 535 24. J. R. Bernhardt, J. M. Sunday, M. I. O'Connor, Metabolic Theory and the Temperature-  
536 Size Rule Explain the Temperature Dependence of Population Carrying Capacity. *Am. Nat.*  
537 **192**, 687–697 (2018).
- 538 25. G. Yvon-Durocher, *et al.*, Reconciling the temperature dependence of respiration across  
539 timescales and ecosystem types. *Nature* **487**, 472–476 (2012).
- 540 26. J. F. Gillooly, J. H. Brown, G. B. West, V. M. Savage, E. L. Charnov, Effects of size and  
541 temperature on metabolic rate. *Science* **293**, 2248–2251 (2001).
- 542 27. C. F. Clements, B. Collen, T. M. Blackburn, O. L. Petchey, Effects of directional  
543 environmental change on extinction dynamics in experimental microbial communities are  
544 predicted by a simple model. *Oikos* **123**, 141–150 (2014).
- 545 28. D. Kirk, *et al.*, Empirical evidence that metabolic theory describes the temperature  
546 dependency of within-host parasite dynamics. *PLoS Biol.* **16**, e2004608 (2018).
- 547 29. A. I. Dell, S. Pawar, V. M. Savage, Systematic variation in the temperature dependence of  
548 physiological and ecological traits. *Proc. Natl. Acad. Sci.* **108**, 10591–10596 (2011).
- 549 30. J. R. Schramski, A. I. Dell, J. M. Grady, R. M. Sibly, J. H. Brown, Metabolic theory predicts  
550 whole-ecosystem properties. *Proc. Natl. Acad. Sci.* **112**, 2617–2622 (2015).
- 551 31. B. J. Enquist, *et al.*, Scaling metabolism from organisms to ecosystems. *Nature* **423**, 639–  
552 642 (2003).
- 553 32. M. Lindmark, J. Ohlberger, M. Huss, A. Gårdmark, Size-based ecological interactions drive  
554 food web responses to climate warming. *Ecol. Lett.* **22**, 778–786 (2019).
- 555 33. G. Sugihara, R. M. May, Nonlinear forecasting as a way of distinguishing chaos from  
556 measurement error in time series. *Nature* **344**, 734–741 (1990).
- 557 34. E. R. Deyle, *et al.*, Predicting climate effects on Pacific sardine. *Proc. Natl. Acad. Sci.* **110**,  
558 6430–6435 (2013).
- 559 35. T. L. Rogers, S. B. Munch, Hidden similarities in the dynamics of a weakly synchronous  
560 marine metapopulation. *Proc. Natl. Acad. Sci.* **117**, 479–485 (2020).
- 561 36. U. Halbach, Population dynamics of rotifers and its consequences for ecotoxicology.  
562 *Hydrobiologia* **109**, 79–96 (1984).

- 563 37. J. P. DeLong, S. Lyon, Temperature alters the shape of predator–prey cycles through  
564 effects on underlying mechanisms. *PeerJ* **8**, e9377 (2020).
- 565 38. K. E. Fussmann, F. Schwarzmüller, U. Brose, A. Jousset, B. C. Rall, Ecological stability in  
566 response to warming. *Nat. Clim. Change* **4**, 206–210 (2014).
- 567 39. A. M. Laughton, R. J. Knell, Warming at the population level: Effects on age structure,  
568 density, and generation cycles. *Ecol. Evol.* **9**, 4403–4420 (2019).
- 569 40. A. Hastings, T. Powell, Chaos in a Three-Species Food Chain. *Ecology* **72**, 896–903  
570 (1991).
- 571 41. G. Wang, M. E. Dillon, Recent geographic convergence in diurnal and annual temperature  
572 cycling flattens global thermal profiles. *Nat. Clim. Change* **4**, 988–992 (2014).
- 573 42. M. J. Angilletta, *Thermal Adaptation: A Theoretical and Empirical Synthesis* (OUP Oxford,  
574 2009).
- 575 43. T. L. Martin, R. B. Huey, Why “Suboptimal” Is Optimal: Jensen’s Inequality and Ectotherm  
576 Thermal Preferences. *Am. Nat.* **171**, E102–E118 (2008).
- 577 44. K. Judd, A. Mees, Embedding as a modeling problem. *Phys. Nonlinear Phenom.* **120**, 273–  
578 286 (1998).
- 579 45. J. Stark, Delay Embeddings for Forced Systems. I. Deterministic Forcing. *J. Nonlinear Sci.*  
580 **9**, 255–332 (1999).
- 581 46. A. C. Iles, Towards predicting community level effects of climate: Relative temperature  
582 scaling of metabolic and ingestion rates. *Ecology* (2014) <https://doi.org/10.1890/13-1342.1>  
583 (February 26, 2014).
- 584 47. N. J. B. Isaac, C. Carbone, Why are metabolic scaling exponents so controversial?  
585 Quantifying variance and testing hypotheses. *Ecol. Lett.* **13**, 728–735.
- 586 48. G. Englund, G. Öhlund, C. L. Hein, S. Diehl, Temperature dependence of the functional  
587 response. *Ecol. Lett.* **14**, 914–921 (2011).
- 588 49. A. Gårdmark, M. Huss, Individual variation and interactions explain food web responses to  
589 global warming. *Philos. Trans. R. Soc. B Biol. Sci.* **375**, 20190449 (2020).
- 590 50. J. J. Elser, *et al.*, Biological stoichiometry from genes to ecosystems. *Ecol. Lett.* **3**, 540–  
591 550 (2000).
- 592 51. A. P. Allen, J. F. Gillooly, Towards an integration of ecological stoichiometry and the  
593 metabolic theory of ecology to better understand nutrient cycling. *Ecol. Lett.* **12**, 369–384  
594 (2009).
- 595 52. J. F. Gillooly, E. L. Charnov, G. B. West, V. M. Savage, J. H. Brown, Effects of size and  
596 temperature on developmental time. *Nature* **417**, 70 (2002).

- 597 53. E. R. Deyle, *et al.*, A hybrid empirical and parametric approach for managing ecosystem  
598 complexity: Water quality in Lake Geneva under nonstationary futures. *Proc. Natl. Acad.*  
599 *Sci.* **119**, e2102466119 (2022).
- 600 54. V. Agarwal, C. C. James, C. E. Widdicombe, A. D. Barton, Intraseasonal predictability of  
601 natural phytoplankton population dynamics. *Ecol. Evol.* **11**, 15720–15739 (2021).
- 602 55. G. Sugihara, *et al.*, Residual delay maps unveil global patterns of atmospheric nonlinearity  
603 and produce improved local forecasts. *Proc. Natl. Acad. Sci.* **96**, 14210–14215 (1999).
- 604 56. J. T. Thorson, K. Ono, S. B. Munch, A Bayesian approach to identifying and compensating  
605 for model misspecification in population models. *Ecology* **95**, 329–341 (2014).
- 606 57. J. Runge, *et al.*, Inferring causation from time series in Earth system sciences. *Nat.*  
607 *Commun.* **10**, 2553 (2019).
- 608 58. J. D. Farmer, J. J. Sidorowich, Predicting chaotic time series. *Phys. Rev. Lett.* **59**, 845–848  
609 (1987).
- 610 59. S. B. Munch, S. Salinas, Latitudinal variation in lifespan within species is explained by the  
611 metabolic theory of ecology. *Proc. Natl. Acad. Sci.* **106**, 13860–13864 (2009).
- 612 60. A. Rohatgi, WebPlotDigitizer (2020).
- 613 61. R. M. Schoolfield, P. J. H. Sharpe, C. E. Magnuson, Non-linear regression of biological  
614 temperature-dependent rate models based on absolute reaction-rate theory. *J. Theor. Biol.*  
615 **88**, 719–731 (1981).
- 616 62. B. K. Sullivan, L. T. McManus, Factors controlling seasonal succession of the copepods  
617 *Acartia hudsonica* and *A. tonsa* in Narragansett Bay, Rhode Island: temperature and  
618 resting egg production (1986).
- 619 63. F. H. Nabetta, M. Nakai, Y. Kunimi, Effects of temperature and photoperiod on the  
620 development and reproduction of *Adoxophyes honmai* (Lepidoptera: Tortricidae). *Appl.*  
621 *Entomol. Zool.* **40**, 231–238 (2005).
- 622  
623

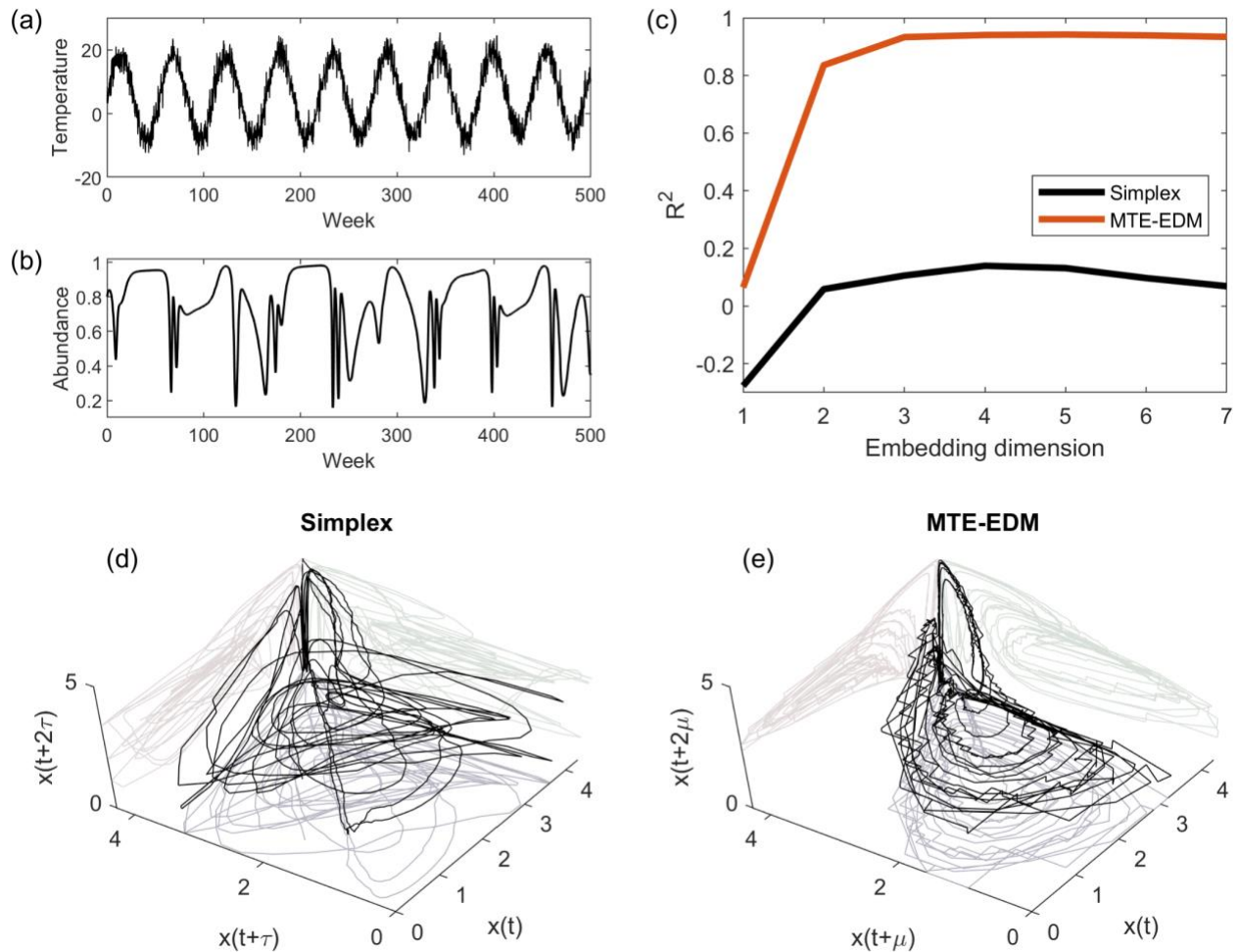




624

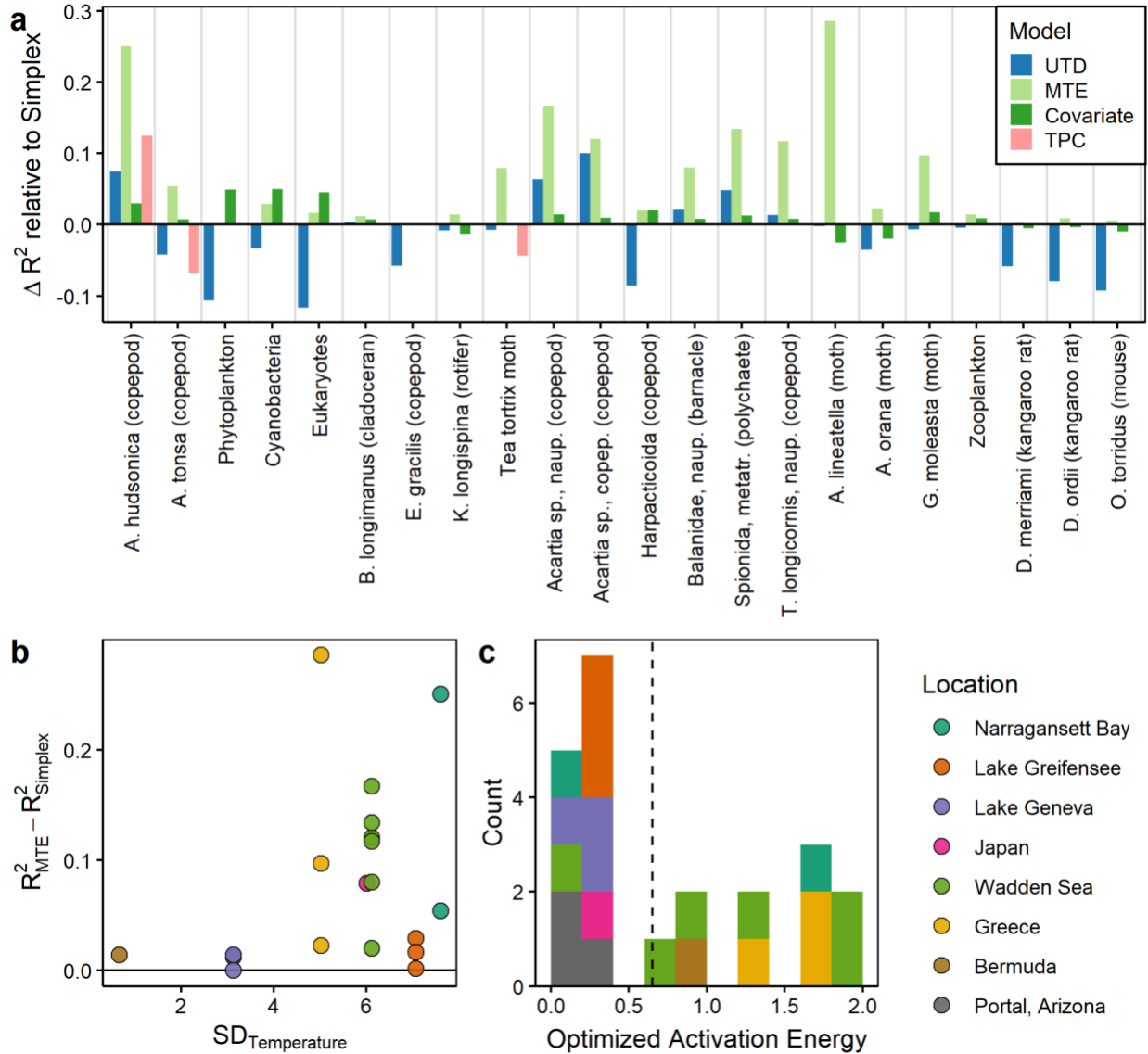
625 **Figure 1.** Conceptual diagrams demonstrating principles behind MTE-EDM and the rescaling of time with  
 626 temperature. The example in (A) and (B) depicts a seasonal system. (A) Calendar time and metabolic  
 627 time proceed at different rates depending on temperature (light blue indicates low temperatures, red high  
 628 temperatures). (B) Abundance dynamics will proceed faster at higher temperatures, but have the same  
 629 underlying dynamics when using a metabolic timestep. A constant metabolic timestep can be achieved  
 630 using a dynamic calendar time step based on temperature. (C) Under the assumptions of MTE-EDM,  
 631 population cycle period should decrease with increasing temperature. Consistent with this assumption,  
 632 empirically-measured cycle periods in constant-temperature laboratory experiments scale with  
 633 temperature. Filled shapes and solid linear regression from (37), open shapes and dashed linear  
 634 regression from (36).

635



636  
 637  
 638  
 639  
 640  
 641

**Figure 2.** Simulated population dynamics with temperature seasonality, a long-term trend, and stochasticity. Panel (a) shows temperature and (b) abundance time series. (c) Leave-one-out prediction  $R^2$  for Simplex and MTE-EDM with different embedding dimensions. (d) Reconstructed attractor in delay-coordinate space using a fixed calendar timestep or (e) using a fixed metabolic timestep.



642  
643

644 **Figure 3.** (a) Change in forecast performance (as measured by change in leave-one-out prediction  $R^2$ ) for  
 645 each model relative to the Simplex, for each empirical time series. Models used a metabolic timestep  
 646 based on either universal temperature dependence (UTD), optimized temperature dependence (MTE), or  
 647 empirical thermal performance curves (TPC), or used a calendar timestep with temperature as a covariate  
 648 (Covariate). Only 3 series had TPC models. Mean  $\pm$  standard deviation for change in  $R^2$  across ectotherm  
 649 series: UTD:  $-0.01 \pm 0.06$ , MTE:  $0.08 \pm 0.08$ , Covariate:  $0.01 \pm 0.02$ . (b) Change in forecast performance  
 650 (MTE vs. Simplex) vs. standard deviation of temperature, excluding endotherms (3 rodent time series  
 651 from Portal, Arizona). (c) Distribution of optimized activation energies from MTE-EDM. The vertical  
 652 dashed line is the UTD value (0.65). The Simplex model (no temperature dependence) corresponds to an  
 653 activation energy of 0. Exact activation energy values are given in **Fig. S5**.  
 654

655 **Table 1.** Metadata for empirical datasets used in the study and leave-one-out  $R^2$  values for Simplex and  
 656 MTE-EDM. Data citations are in **Table S2**.

Taxon		Location	Sampling interval	Time series length (n)	$R^2$ (Simplex)	$R^2$ (MTE-EDM)
<i>Acartia hudsonica</i>	copepod	Narragansett Bay	weekly	767	0.63	0.88
<i>Acartia tonsa</i>	copepod	Narragansett Bay	weekly	767	0.72	0.78
Phytoplankton		Lake Greifensee	monthly	388	0.57	0.57
Cyanobacteria		Lake Greifensee	monthly	388	0.58	0.61
Eukaryotes		Lake Greifensee	monthly	388	0.37	0.39
<i>Bythotrephes longimanus</i>	cladoceran	Lake Geneva	biweekly	1038	0.85	0.86
<i>Eudiaptomus gracilis</i>	copepod	Lake Geneva	biweekly	1038	0.78	0.78
<i>Kellicottia longispina</i>	rotifer	Lake Geneva	biweekly	1038	0.83	0.84
<i>Adoxophyes honmai</i>	moth	Japan	5 days	2754	0.54	0.62
<i>Acartia</i> sp., nauplii	copepod	Wadden Sea	weekly	503	0.48	0.65
<i>Acartia</i> sp., copepodites	copepod	Wadden Sea	weekly	503	0.51	0.63
Harpacticoida	copepod	Wadden Sea	weekly	503	0.66	0.68
Balanidae, nauplii	barnacle	Wadden Sea	weekly	503	0.66	0.74
Spionida, metatrochophora	polychaete	Wadden Sea	weekly	503	0.36	0.50
<i>Temora longicornis</i> , nauplii	copepod	Wadden Sea	weekly	503	0.58	0.70
<i>Anarsia lineatella</i>	moth	Greece	3 days	322	0.22	0.51
<i>Adoxophyes orana</i>	moth	Greece	3 days	322	0.43	0.45
<i>Grapholita moleasta</i>	moth	Greece	3 days	322	0.60	0.70
Zooplankton		Bermuda	biweekly	600	0.49	0.50
<i>Dipodomys merriami</i>	kangaroo rat	Portal, Arizona	monthly	312	0.80	0.80
<i>Dipodomys ordii</i>	kangaroo rat	Portal, Arizona	monthly	312	0.80	0.80
<i>Onychomys torridus</i>	mouse	Portal, Arizona	monthly	312	0.70	0.71

657